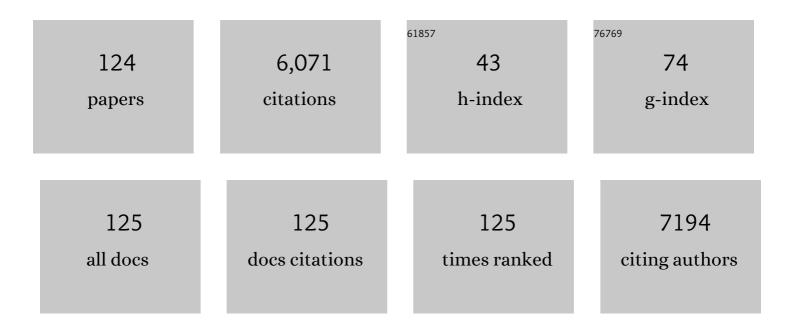
List of Publications by Year in descending order

Source: https://exaly.com/author-pdf/3175869/publications.pdf Version: 2024-02-01



ΙΙΔΝΙΙΙΝ ΤΙΔΝ

#	Article	IF	CITATIONS
1	Improving the Performance and Stability of Perovskite Solar Cells through Buried Interface Passivation Using Potassium Hydroxide. ACS Applied Energy Materials, 2022, 5, 1914-1921.	2.5	11
2	Stable and Efficient Red-Emitting Perovskite Cross-Shaped Nanoplates. Journal of Physical Chemistry Letters, 2022, 13, 1506-1511.	2.1	3
3	Operational Stability Issues and Challenges in Metal Halide Perovskite Light-Emitting Diodes. Journal of Physical Chemistry Letters, 2022, 13, 1962-1971.	2.1	31
4	Electron Delocalization in CsPbI ₃ Quantum Dots Enables Efficient Lightâ€Emitting Diodes with Improved Efficiency Rollâ€Off. Advanced Optical Materials, 2022, 10, .	3.6	16
5	Evolution of magnetoresistance with temperature in the insulating van der Waals compound Ta ₂ Pd ₃ Te ₅ . Applied Physics Letters, 2022, 120, 161901.	1.5	3
6	Exploring performance degradation of quantum-dot light-emitting diodes. Journal of Materials Chemistry C, 2022, 10, 8642-8649.	2.7	9
7	A boosting carrier transfer passivation layer for achieving efficient perovskite solar cells. Journal of Materials Chemistry C, 2022, 10, 9794-9801.	2.7	4
8	Thermally Stable Redâ€Emitting Mixed Halide Perovskite Nanocrystals Enabled by Solid Reaction and Coâ€Doping Process. Advanced Optical Materials, 2022, 10, .	3.6	11
9	Interphases, Interfaces, and Surfaces of Active Materials in Rechargeable Batteries and Perovskite Solar Cells. Advanced Materials, 2021, 33, e1905245.	11.1	30
10	Gradient-Band Alignment Homojunction Perovskite Quantum Dot Solar Cells. Journal of Physical Chemistry Letters, 2021, 12, 1018-1024.	2.1	33
11	Insights into iodoplumbate complex evolution of precursor solutions for perovskite solar cells: from aging to degradation. Journal of Materials Chemistry A, 2021, 9, 6732-6748.	5.2	26
12	Electroluminescence Principle and Performance Improvement of Metal Halide Perovskite Lightâ€Emitting Diodes. Advanced Optical Materials, 2021, 9, 2002167.	3.6	49
13	Perovskite Quantum Dots with Ultralow Trap Density by Acid Etchingâ€Driven Ligand Exchange for High Luminance and Stable Pureâ€Blue Lightâ€Emitting Diodes. Advanced Materials, 2021, 33, e2006722.	11.1	196
14	Induction of Wurtzite to Zinc-Blende Phase Transformation in ZnSe Nanorods During Cu(I) Cation Exchange. Chemistry of Materials, 2021, 33, 2398-2407.	3.2	7
15	Demystifying the Formation of Colloidal Perovskite Nanocrystals via Controlling Stepwise Synthesis. Journal of Physical Chemistry C, 2021, 125, 14204-14211.	1.5	11
16	Highly Pure White Light-Emitting Single-Component Perovskite Colloidal Quantum Dots. Journal of Physical Chemistry C, 2021, 125, 18810-18816.	1.5	8
17	Multiple-Function Surface Engineering of SnO ₂ Nanoparticles to Achieve Efficient Perovskite Solar Cells. Journal of Physical Chemistry Letters, 2021, 12, 9142-9148.	2.1	19
18	Filtering Strategy of Colloidal Quantum Dots for Improving Performance of Light-Emitting Diodes. Journal of Physical Chemistry C, 2021, 125, 2299-2305.	1.5	4

#	Article	IF	CITATIONS
19	Highâ€Quality αâ€FAPbI ₃ Film Assisted by Lead Acetate for Efficient Solar Cells. Solar Rrl, 2021, 5, 2100747.	3.1	10
20	Combined <i>in Situ</i> Photoluminescence and X-ray Scattering Reveals Defect Formation in Lead-Halide Perovskite Films. Journal of Physical Chemistry Letters, 2021, 12, 10156-10162.	2.1	15
21	High Efficiency and Narrow Emission Band Pure-Red Perovskite Colloidal Quantum Wells. Journal of Physical Chemistry Letters, 2021, 12, 10735-10741. Absence of long-range magnetic order in <mml:math< td=""><td>2.1</td><td>14</td></mml:math<>	2.1	14
22	xmlns:mml="http://www.w3.org/1998/Math/MathML"> <mml:msub><mml:mi mathvariant="normal">Fe<mml:mrow><mml:mn>1</mml:mn><mml:mo>â^`</mml:mo><mml:mi>î mathvariant="normal">Te</mml:mi><mml:mn>2</mml:mn></mml:mrow></mml:mi </mml:msub> (<mml:math) etqq0<="" td="" tj=""><td>nml:mi>< 0 0 rgBT /</td><td>/mml:mrow>< /Overlock 10 T</td></mml:math)>	nml:mi>< 0 0 rgBT /	/mml:mrow>< /Overlock 10 T
23	Controllable Ferromagnetism in Super-tetragonal PbTiO ₃ through Strain Engineering. Nano Letters, 2020, 20, 881-886.	4.5	11
24	Photoelectrochemical Performance Enhancement of ZnSe Nanorods versus Dots: Combined Experimental and Computational Insights. Journal of Physical Chemistry Letters, 2020, 11, 10414-10420.	2.1	5
25	Selfâ€Assembled Perovskite Nanowire Clusters for High Luminance Red Lightâ€Emitting Diodes. Advanced Functional Materials, 2020, 30, 2005990.	7.8	67
26	Gradient Annealing of Halide Perovskite Films for Improved Performance of Solar Cells. ACS Applied Energy Materials, 2020, 3, 8130-8134.	2.5	6
27	Double Active Layers Constructed with Halide Perovskite and Quantum Dots for Broadband Photodetection. Advanced Optical Materials, 2020, 8, 2000557.	3.6	19
28	Atomic Sulfur Passivation Improves the Photoelectrochemical Performance of ZnSe Nanorods. Nanomaterials, 2020, 10, 1081.	1.9	5
29	CsPbl ₃ /PbSe Heterostructured Nanocrystals for High-Efficiency Solar Cells. ACS Energy Letters, 2020, 5, 2401-2410.	8.8	77
30	Stable CsPb _{1–<i>x</i>} Zn <i>_x</i> ₃ Colloidal Quantum Dots with Ultralow Density of Trap States for High-Performance Solar Cells. Chemistry of Materials, 2020, 32, 6105-6113.	3.2	93
31	Controlled crystallinity and morphologies of 2D Ruddlesden-Popper perovskite films grown without anti-solvent for solar cells. Chemical Engineering Journal, 2020, 394, 124959.	6.6	33
32	Exploiting Flexible Memristors Based on Solutionâ€Processed Colloidal CuInSe ₂ Nanocrystals. Advanced Electronic Materials, 2020, 6, 2000035.	2.6	10
33	Engineering Halide Perovskite Crystals through Precursor Chemistry. Small, 2019, 15, e1903613.	5.2	82
34	Spray oated Colloidal Perovskite Quantum Dot Films for Highly Efficient Solar Cells. Advanced Functional Materials, 2019, 29, 1906615.	7.8	100
35	Ultra-long photoluminescence lifetime in an inorganic halide perovskite thin film. Journal of Materials Chemistry A, 2019, 7, 22229-22234.	5.2	23
36	Synthesis of Colloidal Blue-Emitting InP/ZnS Core/Shell Quantum Dots with the Assistance of Copper Cations. Journal of Physical Chemistry Letters, 2019, 10, 6720-6726.	2.1	26

#	Article	IF	CITATIONS
37	Stable and Strong Emission CsPbBr ₃ Quantum Dots by Surface Engineering for High-Performance Optoelectronic Films. ACS Applied Materials & Interfaces, 2019, 11, 25410-25416.	4.0	91
38	Spontaneous Selfâ€Assembly of Cesium Lead Halide Perovskite Nanoplatelets into Cuboid Crystals with High Intensity Blue Emission. Advanced Science, 2019, 6, 1900462.	5.6	69
39	Fe doping enhances ferromagnetism in MgTiO3 films. Journal of Materials Science: Materials in Electronics, 2019, 30, 10499-10506.	1.1	3
40	Improved Stability and Photodetector Performance of CsPbI ₃ Perovskite Quantum Dots by Ligand Exchange with Aminoethanethiol. Advanced Functional Materials, 2019, 29, 1902446.	7.8	206
41	Enhanced-performance of self-powered flexible quantum dot photodetectors by a double hole transport layer structure. Nanoscale, 2019, 11, 9626-9632.	2.8	18
42	Dip-coated colloidal quantum-dot films for high-performance broadband photodetectors. Journal of Materials Chemistry C, 2019, 7, 6266-6272.	2.7	21
43	Perovskite CsPbBr3 Quantum Dots Prepared Using Discarded Lead–Acid Battery Recycled Waste. Energies, 2019, 12, 1117.	1.6	11
44	Fe _{0.36(4)} Pd _{0.64(4)} Se ₂ : Magnetic Spin-Glass Polymorph of FeSe ₂ and PdSe ₂ Stable at Ambient Pressure. Inorganic Chemistry, 2019, 58, 3107-3114.	1.9	4
45	Thermally Stable Copper(II)-Doped Cesium Lead Halide Perovskite Quantum Dots with Strong Blue Emission. Journal of Physical Chemistry Letters, 2019, 10, 943-952.	2.1	274
46	Spray Coated Colloidal Quantum Dot Films for Broadband Photodetectors. Nanomaterials, 2019, 9, 1738.	1.9	10
47	From scalable solution fabrication of perovskite films towards commercialization of solar cells. Energy and Environmental Science, 2019, 12, 518-549.	15.6	269
48	Broadband hybrid organic/CuInSe ₂ quantum dot photodetectors. Journal of Materials Chemistry C, 2018, 6, 2573-2579.	2.7	44
49	Room-Temperature Construction of Mixed-Halide Perovskite Quantum Dots with High Photoluminescence Quantum Yield. Journal of Physical Chemistry C, 2018, 122, 5151-5160.	1.5	79
50	Original Core–Shell Structure of Cubic CsPbBr ₃ @Amorphous CsPbBr _{<i>x</i>} Perovskite Quantum Dots with a High Blue Photoluminescence Quantum Yield of over 80%. ACS Energy Letters, 2018, 3, 245-251.	8.8	202
51	Tuning optical and magnetic properties of nanocrystalline BaTiO3 films by Fe doping. Applied Physics A: Materials Science and Processing, 2018, 124, 1.	1.1	8
52	CuInSe ₂ Quantum Dots Hybrid Hole Transfer Layer for Halide Perovskite Photodetectors. ACS Applied Materials & Interfaces, 2018, 10, 35656-35663.	4.0	30
53	Repairing Defects of Halide Perovskite Films To Enhance Photovoltaic Performance. ACS Applied Materials & Interfaces, 2018, 10, 37005-37013.	4.0	40
54	Significant Stability Enhancement of Perovskite Solar Cells by Facile Adhesive Encapsulation. Journal of Physical Chemistry C, 2018, 122, 25260-25267.	1.5	31

#	Article	IF	CITATIONS
55	Hierarchical ZnO microspheres photoelectrodes assembled with Zn chalcogenide passivation layer for high efficiency quantum dot sensitized solar cells. Journal of Power Sources, 2018, 401, 255-262.	4.0	15
56	Monolayer-like hybrid halide perovskite films prepared by additive engineering without antisolvents for solar cells. Journal of Materials Chemistry A, 2018, 6, 15386-15394.	5.2	53
57	Surface Trap States Passivation for Highâ€Performance Inorganic Perovskite Solar Cells. Solar Rrl, 2018, 2, 1800188.	3.1	103
58	Surface Engineering of Quantum Dots for Remarkably High Detectivity Photodetectors. Journal of Physical Chemistry Letters, 2018, 9, 3285-3294.	2.1	31
59	High-Voltage-Efficiency Inorganic Perovskite Solar Cells in a Wide Solution-Processing Window. Journal of Physical Chemistry Letters, 2018, 9, 3646-3653.	2.1	63
60	Continuous Size Tuning of Monodispersed ZnO Nanoparticles and Its Size Effect on the Performance of Perovskite Solar Cells. ACS Applied Materials & amp; Interfaces, 2017, 9, 9785-9794.	4.0	43
61	Controlled growth of Cu3Se2 nanosheets array counter electrode for quantum dots sensitized solar cell through ion exchange. Science China Materials, 2017, 60, 637-645.	3.5	27
62	Highly Efficient and Stable Perovskite Solar Cells Based on Monolithically Grained CH ₃ NH ₃ PbI ₃ Film. Advanced Energy Materials, 2017, 7, 1602017.	10.2	291
63	Colloidal engineering for monolayer CH ₃ NH ₃ PbI ₃ films toward high performance perovskite solar cells. Journal of Materials Chemistry A, 2017, 5, 24168-24177.	5.2	87
64	Monolithic MAPbI ₃ films for high-efficiency solar cells via coordination and a heat assisted process. Journal of Materials Chemistry A, 2017, 5, 21313-21319.	5.2	132
65	An air-stable ultraviolet photodetector based on mesoporous TiO ₂ /spiro-OMeTAD. Journal of Materials Chemistry C, 2017, 5, 10543-10548.	2.7	26
66	Titanium dioxide nanowires modified tin oxide hollow spheres for dye-sensitized solar cells. MRS Communications, 2016, 6, 226-233.	0.8	6
67	A structure of CdS/CuxS quantum dots sensitized solar cells. Applied Physics Letters, 2016, 108, 213901.	1.5	25
68	Novel Photoanode for Dye-Sensitized Solar Cells with Enhanced Light-Harvesting and Electron-Collection Efficiency. ACS Applied Materials & Interfaces, 2016, 8, 13418-13425.	4.0	38
69	Impact of sol aging on TiO2 compact layer and photovoltaic performance of perovskite solar cell. Science China Materials, 2016, 59, 710-718.	3.5	23
70	Critical current density and vortex pinning in tetragonalFeS1â^'xSex(x=0,0.06). Physical Review B, 2016, 94, .	1.1	18
71	Constructing water-resistant CH ₃ NH ₃ PbI ₃ perovskite films via coordination interaction. Journal of Materials Chemistry A, 2016, 4, 17018-17024.	5.2	89
72	Cu ₃ Se ₂ nanostructure as a counter electrode for high efficiency quantum dot-sensitized solar cells. Journal of Materials Chemistry C, 2016, 4, 8020-8026.	2.7	42

#	Article	IF	CITATIONS
73	Ultrathin ALD coating on TiO2 photoanodes with enhanced quantum dot loading and charge collection in quantum dots sensitized solar cells. Science China Materials, 2016, 59, 833-841.	3.5	21
74	Recent advances in counter electrodes of quantum dot-sensitized solar cells. RSC Advances, 2016, 6, 90082-90099.	1.7	41
75	Enhanced Performance of PbS-quantum-dot-sensitized Solar Cells via Optimizing Precursor Solution and Electrolytes. Scientific Reports, 2016, 6, 23094.	1.6	69
76	Optical properties of Fe-doped BaTiO3 films deposited on quartz substrates by sol-gel method. Journal of Alloys and Compounds, 2016, 687, 529-533.	2.8	10
77	Controlled growth of textured perovskite films towards high performance solar cells. Nano Energy, 2016, 27, 17-26.	8.2	123
78	Dynamic Growth of Pinhole-Free Conformal CH3NH3PbI3 Film for Perovskite Solar Cells. ACS Applied Materials & Interfaces, 2016, 8, 4684-4690.	4.0	50
79	Investigation of the role of Mn dopant in CdS quantum dot sensitized solar cell. Electrochimica Acta, 2016, 191, 62-69.	2.6	49
80	Design, fabrication and modification of metal oxide semiconductor for improving conversion efficiency of excitonic solar cells. Coordination Chemistry Reviews, 2016, 320-321, 193-215.	9.5	56
81	Magnetic and optical properties of La-doped BiFeO3 films prepared by sol–gel route. Journal of Materials Science: Materials in Electronics, 2015, 26, 700-704.	1.1	16
82	Effects of Fe doping on the optical and magnetic properties of TiO2 films deposited on Si substrates by a sol–gel route. Journal of Sol-Gel Science and Technology, 2015, 74, 521-527.	1.1	6
83	Dye-sensitized solar cells based on hierarchically structured porous TiO ₂ filled with nanoparticles. Journal of Materials Chemistry A, 2015, 3, 11320-11329.	5.2	34
84	Control of Nanostructures and Interfaces of Metal Oxide Semiconductors for Quantum-Dots-Sensitized Solar Cells. Journal of Physical Chemistry Letters, 2015, 6, 1859-1869.	2.1	102
85	Rapid construction of TiO ₂ aggregates using microwave assisted synthesis and its application for dye-sensitized solar cells. RSC Advances, 2015, 5, 8622-8629.	1.7	49
86	Improved charge generation and collection in dye-sensitized solar cells with modified photoanode surface. Nano Energy, 2014, 10, 353-362.	8.2	38
87	A highly efficient (>6%) Cd _{1â^'x} Mn _x Se quantum dot sensitized solar cell. Journal of Materials Chemistry A, 2014, 2, 19653-19659.	5.2	126
88	Microwave-Assisted Synthesis of SnO ₂ Nanosheets Photoanodes for Dye-Sensitized Solar Cells. Journal of Physical Chemistry C, 2014, 118, 25931-25938.	1.5	42
89	Enhanced magnetoelectric effect in magnetostrictive/piezoelectric laminates through adopting magnetic warm compaction Terfenol-D. Journal of Alloys and Compounds, 2014, 587, 287-289.	2.8	18
90	Rare earth elements recycling from waste phosphor by dual hydrochloric acid dissolution. Journal of Hazardous Materials, 2014, 272, 96-101.	6.5	63

#	Article	IF	CITATIONS
91	Microsphere Light-Scattering Layer Assembled by ZnO Nanosheets for the Construction of High Efficiency (>5%) Quantum Dots Sensitized Solar Cells. Journal of Physical Chemistry C, 2014, 118, 16611-16617.	1.5	47
92	Hierarchically Structured ZnO Nanorods–Nanosheets for Improved Quantum-Dot-Sensitized Solar Cells. ACS Applied Materials & Interfaces, 2014, 6, 4466-4472.	4.0	85
93	Nanorod–nanosheet hierarchically structured ZnO crystals on zinc foil as flexible photoanodes for dye-sensitized solar cells. Nanoscale, 2013, 5, 1894.	2.8	42
94	Sn-Doped V ₂ O ₅ Film with Enhanced Lithium-Ion Storage Performance. Journal of Physical Chemistry C, 2013, 117, 23507-23514.	1.5	170
95	Influence of Cationic Precursors on CdS Quantum-Dot-Sensitized Solar Cell Prepared by Successive Ionic Layer Adsorption and Reaction. Journal of Physical Chemistry C, 2013, 117, 26948-26956.	1.5	76
96	Influence of transition metal doping on the structural, optical, and magnetic properties of TiO2 films deposited on Si substrates by a sol–gel process. Nanoscale Research Letters, 2013, 8, 533.	3.1	52
97	A ZnO nanorod layer with a superior light-scattering effect for dye-sensitized solar cells. RSC Advances, 2013, 3, 18537.	1.7	23
98	Structural, magnetic and optical properties of Ni-doped TiO2 thin films deposited on silicon(100) substrates by sol–gel process. Journal of Alloys and Compounds, 2013, 581, 318-323.	2.8	63
99	Architecturing high magnetic properties of NdFeB/SmFeN hybrid magnets. Materials Letters, 2013, 105, 87-89.	1.3	15
100	ZnO nanocrystallite aggregates synthesized through interface precipitation for dye-sensitized solar cells. Nano Energy, 2013, 2, 40-48.	8.2	43
101	Constructing ZnO nanorod array photoelectrodes for highly efficient quantum dot sensitized solar cells. Journal of Materials Chemistry A, 2013, 1, 6770.	5.2	74
102	ZnO/TiO ₂ nanocable structured photoelectrodes for CdS/CdSe quantum dot co-sensitized solar cells. Nanoscale, 2013, 5, 936-943.	2.8	124
103	Architectured ZnO photoelectrode for high efficiency quantum dot sensitized solar cells. Energy and Environmental Science, 2013, 6, 3542.	15.6	116
104	Copper nanocrystal modified activated carbon for supercapacitors with enhanced volumetric energy and power density. Journal of Power Sources, 2013, 236, 215-223.	4.0	44
105	CdS/CdSe Quantum Dot Co-sensitized Solar Cells. , 2013, , .		0
106	Semiconductor quantum dot-sensitized solar cells. Nano Reviews, 2013, 4, 22578.	3.7	109
107	Enhanced Performance of CdS/CdSe Quantum Dot Cosensitized Solar Cells via Homogeneous Distribution of Quantum Dots in TiO ₂ Film. Journal of Physical Chemistry C, 2012, 116, 18655-18662.	1.5	176
108	Influence of Ni doping on phase transformation and optical properties of TiO2 films deposited on quartz substrates by sol–gel process. Applied Surface Science, 2012, 258, 4893-4897.	3.1	11

#	Article	IF	CITATIONS
109	Co-reduction synthesis of uniform ferromagnetic SmCo nanoparticles. Materials Letters, 2012, 68, 212-214.	1.3	20
110	Effects of Co doping on structure and optical properties of TiO2 thin films prepared by sol–gel method. Thin Solid Films, 2012, 520, 5179-5183.	0.8	30
111	Heat treatment effects on Fe3O4 nanoparticles structure and magnetic properties prepared by carbothermal reduction. Journal of Alloys and Compounds, 2011, 509, 2316-2319.	2.8	72
112	Mn–Zn soft magnetic ferrite nanoparticles synthesized from spent alkaline Zn–Mn batteries. Journal of Alloys and Compounds, 2011, 509, 3991-3994.	2.8	40
113	Effects of Co doping on the phase transformation and optical properties of TiO2 thin films by sol–gel method. Physica E: Low-Dimensional Systems and Nanostructures, 2011, 44, 550-554.	1.3	9
114	Bonded Terfenol-D composites with low eddy current loss and high magnetostriction. Rare Metals, 2010, 29, 579-582.	3.6	5
115	Carbothermal reduction method for Fe3O4 powder synthesis. Journal of Alloys and Compounds, 2010, 502, 338-340.	2.8	36
116	Magnetic properties and thermal stability of anisotropic bonded Nd-Fe-B magnets by warm compaction. Rare Metals, 2009, 28, 245-247.	3.6	2
117	Radial cracks and fracture mechanism of radially oriented ring 2:17 type SmCo magnets. Journal of Alloys and Compounds, 2009, 476, 98-101.	2.8	5
118	Anisotropic bonded NdFeB magnets with radial oriented magnetization by 2-step warm compaction process. Journal of Alloys and Compounds, 2009, 477, 510-514.	2.8	17
119	2:17-type SmCo magnets prepared by powder injection molding using a water-based binder. Journal of Magnetism and Magnetic Materials, 2008, 320, 2168-2171.	1.0	6
120	Behavior of residual carbon in Sm(Co, Fe, Cu, Zr)z permanent magnets. Journal of Alloys and Compounds, 2007, 440, 89-93.	2.8	9
121	Effect of WC particle size on the microstructure, mechanical properties and fracture behavior of WC–(W, Ti, Ta) C–6wt% Co cemented carbides. International Journal of Refractory Metals and Hard Materials, 2007, 25, 405-410.	1.7	32
122	Magnetic properties and microstructure of radially oriented Sm(Co,Fe,Cu,Zr)z ring magnets. Materials Letters, 2007, 61, 5271-5274.	1.3	5
123	Antioxidation Study of Sm(Co, Cu, Fe, Zr)z-Sintered Permanent Magnets by Metal Injection Molding. Journal of Rare Earths, 2006, 24, 569-573.	2.5	6
124	Nucleation Temperatureâ€Dependent Synthesis of Polytypic CuInSe ₂ Nanostructures with Variable Tetrapod‣ike and Coreâ€Shell Morphologies. ChemNanoMat, 0, , .	1.5	1